RSC Advances

This is an *Accepted Manuscript*, which has been through the Royal Society of Chemistry peer review process and has been accepted for publication.

Accepted Manuscripts are published online shortly after acceptance, before technical editing, formatting and proof reading. Using this free service, authors can make their results available to the community, in citable form, before we publish the edited article. This *Accepted Manuscript* will be replaced by the edited, formatted and paginated article as soon as this is available.

You can find more information about *Accepted Manuscripts* in the Information for Authors.

Please note that technical editing may introduce minor changes to the text and/or graphics, which may alter content. The journal's standard Terms & Conditions and the Ethical guidelines still apply. In no event shall the Royal Society of Chemistry be held responsible for any errors or omissions in this *Accepted Manuscript* or any consequences arising from the use of any information it contains.

ROYAL SOCIETY OF CHEMISTRY

www.rsc.org/advances

The ^{13}C chemical shifts changes and exothermic response for MAA/ERY-A binding in the absence and presence of $NH_3 \cdot H_2O$ indicate adding of $NH_3 \cdot H_2O$ is able to prevent the electrostatic interaction between MAA and ERY-A and consequently prevent nonspecific adsorption and achieve higher specificity.

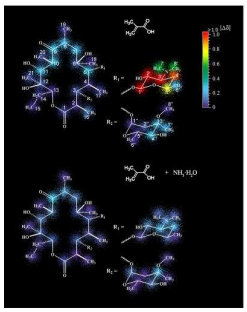

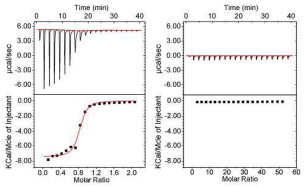

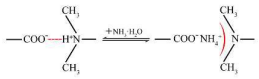

RSC Advances Accepted Manuscript

Journal Name

ARTICLE

Effect of the solvent on improving the recognition properties of surface molecularly imprinted polymers for precise separation of erythromycin

Received 00th January 20xx,
Accepted 00th January 20xx

DOI: 10.1039/x0xx00000x

www.rsc.org/

Yuxin Zhang,[abc] Xue Qu,[ac] FeiFei Wang,[c] Gang Wu,[c] Jinyang Li,[c] Hua Hong,[c] and Changsheng Liu*[abc]

The Formation of thin films with imprinting sites that can be accessed more rapidly by target molecules is an improvement in the bulk molecular imprinting polymers. To achieve suitable properties for specific application, on the basis of our previous study of bulk erythromycin (ERY) imprinted polymers, we here rationally design, generate and test surface-imprinted polymers specific for ERY. ERY-A surface-imprinted glass fibers (GF-MIPs) were fabricated using glass fibers as the matrix, methacrylic acid (MAA) as the functional monomer, ethyleneglycol dimethacrylate (EGDMA) as the cross-linker and azobis(4-cyanovaleric acid) as the initiator. Then, we specifically studied the effect of the solvent on the recognition performance of the GF-MIPs. ^{13}C-NMR and isothermal titration calorimetry (ITC) measurements were employed to demonstrate that the addition of $NH_3{\cdot}H_2O$ can block the interactions between the –COOH group and the tertiary amine on ERY-A. The results of static adsorption and dynamic separation experiments also indicate that an increase of specificity can easily be obtained by mediating the solvent environment, thus satisfying the more stringent requirements of precise separation.

Introduction

The precise separation of target molecules is one of the most critical operations for medicine production because the coexistence of impurities reduces the therapeutic efficiency of medicines or even increases the risk of unpleasant side effects[1,2]. Usually, these impurities contain isomers or derivatives with chemical structures highly similar to the chemical structures of the targets. The removal of such companions is therefore a formidable challenge for precise separation[3,4]. Several advanced technologies, including supercritical fluid extraction[5,6], efficient countercurrent chromatography[7], molecular distillation[8], etc., have been developed to achieve good separation. However, the equipment, energy, and solvent requirements as well as the resultant waste disposal restrict the widespread industrial application of such methods. Alternatively, adsorbents containing specific binding sites for targeting molecules offer strong potential for precise separation. Inspired by the receptor-ligand molecular recognition that occurs in biological systems, chemists have designed molecularly imprinted polymers (MIPs) that exhibit molecular recognition properties[9–11]. MIPs are usually prepared through polymerization of suitable functional monomers in the presence of target molecules (templates). The monomers and templates are pre-organized via various intermolecular interactions such as H-bonding, hydrophobic interactions, van der Waals force and electrostatic interaction. After polymerization and subsequent template removal, imprinted cavities are created that can provide sterically complementary voids and intermolecular forces for template-specific rebinding.

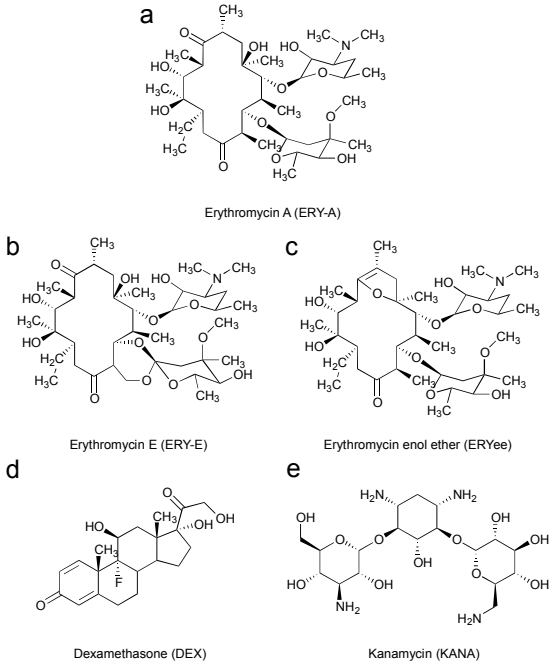

Fig. 1 Chemical structures of (a) erythromycin A (ERY-A), (b) erythromycin E(ERY-E) , (c) erythromycin enol ether (ERYee), (d) dexamethasone (DEX) and (e) kanamycin (KANA).

[a] *The State Key Laboratory of Bioreactor Engineering, East China University of Science and Technology, Shanghai 200237, PR China.*
[b] *Key Laboratory for Ultrafine Materials of Ministry of Education, East China University of Science and Technology, Shanghai 200237, PR China.*
[c] *Engineering Research Centre for Biomedical Materials of Ministry of Education, East China University of Science and Technology, Shanghai 200237, PR China.*

RSC Advances Accepted Manuscript

Please do not adjust margins

Erythromycin (ERY) is a collection of macrolide compounds produced by *Saccharopolyspora erythrae*. ERY-A is an active ingredient with the highest antibacterial activity among the erythromycins[12]. In our previous work, we demonstrated methacrylic acid (MAA) to be the optimal functional monomer for ERY imprinting because MAA can provide multiple H-binding and strong electrostatic interactions for the ERY template[13]. Compared to non-imprinted materials, the generated imprinted adsorbents extracted ERY from its industrial crystal mother liquor with greater specificity. However, this separation was still considered unsatisfactory because, in addition to ERY-A, ERY derivatives such as ERY-E and erythromycin enol ether (ERYee) also remained in the final extracts. The chemical structures of these three ERY compounds in Fig. 1 indicate that all of them have highly similar structures, and contain a tertiary amine group that can interact with MAA via electrostatic interaction. Unlike oriented H-binding, electrostatic interaction has been reported to have no direction that would arouse nonspecific binding, which is probably one of the reasons that precise separation cannot be achieved[14].

The nature of the solvent used for the binding process can substantially influence the expression of specificity[15–17]. For example, strong polar solvents have been reported to weaken the H-binding interactions between MIPs and the template[18,19]. Protic solvent may also influence the electrostatic interaction, and protic solvents with high dielectric constants have been verified to interfere in the formation of functional monomers-template complexes[20,21]. Several researchers have employed the solvent effect to mediate the binding selectivity of the adsorbents. For example, the effect of the polarity of the environment on molecular recognition ability, the variation of polymer recognition properties caused by the change of buffer concentration, pH and presence of organic solvents and the effect of the water content of the selected washing solvent on the recovery of MIP have been studied[22–24]. Therefore, appropriate solvents can be used to achieve precise separation in structurally similar complexes, i.e., ERY systems.

In this study, we propose a strategy to block electrostatic interactions between MAA-based MIPs and ERY by utilizing a solvent containing $NH_3{\cdot}H_2O$. We synthesized ERY-A surface-imprinted glass fibers GF-MIPs using MAA as a functional monomer and EGDMA as a cross-linker. We performed ^{13}C-NMR and isothermal titration calorimetry (ITC) measurement to demonstrate that the addition of $NH_3{\cdot}H_2O$ can block the interactions between MAA and the tertiary amine of ERY-A. Static adsorption and dynamic separation experiments indicate that the imprinting factor and the selectivity of GF-MIPs for ERY-A are improved when an amount of $NH_3{\cdot}H_2O$ is added to the solvents. The results indicate that increasing the recognition accuracy of MIPs by simply mediating the solvent environment is feasible: this increased recognition accuracy would affect biomedical separation and diagnostics applications that require precise recognition.

Experimental

Materials

The ERY standards and "ERY crystal mother solution" were obtained from HEC Pharm Co., Ltd. (Yichang, China). Glass fibers (GF) were purchased from Corker Composite Materials Co., Ltd. (Hangzhou, China). 3-Aminopropyltriethoxysilane (APTS), 1-(3-dimethylaminopropyl)-3-ethylcarbodiimide hydrochloride (EDCI), 1-hydroxybenzotriazole (HOBT), triethylamine (TEA) and 4,4'-azobis (4-cyanovaleric acid) (ACPA) were purchased from Jingchun Reagent Co., Ltd. (Shanghai, China). All other reagents were of analytical grade and were purchased from China Nation Medicines (Shanghai, China).

The "crystal mother solution" is the residual liquid from the ERY crystallization process in industrial production, which includes small amounts of ERY-A and other ERY derivatives, some inorganic matter and other unidentified impurities. The solvent is a 5-10% acetone-water mixture.

Preparation of grafted fibers GF-ACPA

GF were soaked in hot alkali solution for 3 h before use. The coupling agent, APTS, was grafted onto the GFs through a common method in toluene[25]. The amino-modified GF (amino-GF) barely exhibited adsorption of ERY (Fig. S1) and was preserved in a desiccator for further use.

ACPA (0.60 g) was dissolved in dichloromethane in a three-neck flask in an ice-salt bath, followed by the addition of 0.98 g of EDCI, 0.69 g of HOBT and 1.04 g of TEA. After 1 h of stirring, 3.00 g of amino-GF were added to the solution and the temperature of the bath was increased to 20 °C for 12 h. Then, the fibers were rinsed successively with dichloromethane, ethanol and water. After the fibers were dried under vacuum, initiator-grafted fibers GF-ACPA were obtained.

Synthesis of surface molecularly imprinted GF (GF-MIPs)

Like most investigations related to imprinting ERY[26,27], MAA and EGDMA were used as the functional monomer and the cross-linking monomer, respectively, in our work. The main procedure was as follow:

Modified fibers GF-ACPA (3.00 g) were added into a three-neck flask containing 100 mL of a mixed solvent of acetonitrile, followed by the addition of 0.44 g of ERY-A, 0.21 g of MAA and 2.2 g of EGDMA. The mixture was stirred constantly and purged with nitrogen gas for 1 h. The polymerization was then performed at 60 °C for 16 h. Thereafter, the template molecule was extracted from the resulting fibers by sequential washing with a methanol and acetic acid (v/v=9:1) solution followed by washing with methanol until no residue of ERY-A was observed in the rinse solution. Finally, the purified GF-MIPs were dried under vacuum. The non-imprinted GF-NIPs were prepared according to the same procedure, except for the addition of the ERY-A template.

Static adsorption experiments

GF-MIPs and GF-NIPs (30 mg) were mixed with ERY-A standard solution in a concentration range of 0.27-2.18 μmol·mL^{-1}. The concentration of the free ERY-A in the supernatant was measured by high performance liquid chromatography (HPLC)[13]. The equilibrium adsorption amount (Q_e) of ERY-A bound to the fibers was determined by subtracting the amount of free ERY-A from the

RSC Advances Accepted Manuscript

This journal is © The Royal Society of Chemistry 20xx

Please do not adjust margins

amount of ERY-A initially added. The theoretical maximum adsorption capacity, Q_m, was calculated according to a Langmuir isotherm model. The Langmuir isotherm is governed by the following equation:

$$Q_e = \frac{Q_m k C_e}{1 + k C_e} \quad (1)$$

where Q_e and C_e are the equilibrium concentration of ERY-A on the adsorbent and in solution, respectively; Q_m and K are the maximum adsorption capacity and equilibrium constant, respectively.

The imprinting factor, *IF*, was used to demonstrate the difference in adsorption capacity between GF-MIPs and GF-NIPs for ERY-A. The *IF* was calculated according to the following equation:

$$IF = \frac{Q_{m_{GF-MIPs}}}{Q_{m_{GF-NIPs}}} \quad (2)$$

The specific adsorption capacity of GF-MIPs was investigated using kanamycin (KANA) and dexamethasone (DEX) for comparisons. The static adsorption tests of GF-MIPs and GF-NIPs for KANA and DEX were carried out mutually independently.

^{13}C NMR studies

Our prior research suggests that ^{13}C NMR spectroscopy can be used to validate the interactions between the functional monomers and ERY[13]. ^{13}C-NMR spectra of the ERY-A and MAA monomer mixture in an acetonitrile-d_3 and deuteroxide (v/v = 4:6) solution were obtained on a NMR spectrometer (AVANCE III 400 MHz, Bruker, Germany). The values of the ^{13}C chemical shift change ($\Delta\delta$) in ERY-A monomer as it interacted with the functional monomer MAA were calculated.

Effect of electrostatic interaction

$NH_3{\cdot}H_2O$ was chosen as a blocker to block the electrostatic interaction between ERY and MAA. All procedures were the same as those in the static adsorption experiment, except that 1.05 (eq.) of $NH_3{\cdot}H_2O$ was added to the ERY-A solution relative to the molar amount of –COOH groups on the materials.

Furthermore, the effects of additional $NH_3{\cdot}H_2O$ on the electrostatic interaction were verified by isothermal titration calorimetry (ITC 200, Microcal, USA). All binding experiments were performed in solutions corresponding to those from previous adsorption experiments. In individual titrations, 2.0 μL of MAA (10 mM) was added from a microsyringe at intervals of 2 min into ERY-A solution (1 mM, 200 μL). All measurements were performed at 25 °C, with the microsyringe stirring at 1500 rpm. Control experiments were performed by injecting the MAA, along with additional $NH_3{\cdot}H_2O$, into an ERY-A solution.

Dynamic separation experiments

A given amount (3.0 g) of GF-MIPs were packed into an empty chromatographic column (5.0 cm × Ø1.0 cm). The powders obtained from vacuum drying of the "ERY crystal mother solution" were dissolved in acetonitrile/water (v/v = 6:4, containing 0.1% of $NH_3{\cdot}H_2O$) to prepare a 0.68 μmol·mL^{-1} solution. Then, the solution was allowed to pass through the column at a rate of 0.31 BV·h^{-1} in succession. The effluents were collected at 1 h interval, and the samples were subsequently subjected to HPLC analysis using a C18 column and quantified using a detection wavelength of 210 nm. Finally, the concentrations of ERY-A, ERY-E and ERYee in each sample were calculated.

Results and discussion

For the synthesis of surface-imprinted polymers, the initiator ACPA was first grafted onto GF. Then, the polymers were allowed to polymerize onto the GF using a "grafting from" approach to promote the increase in effective imprinting sites and avoid undesired polymerization in solution[28,29].

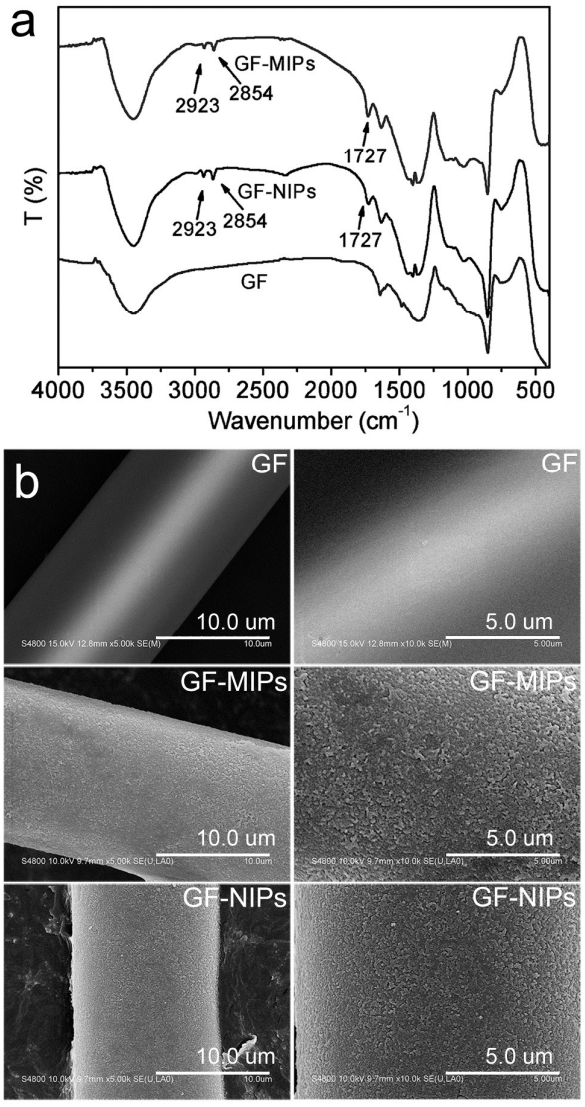

Fig. 2 (a) FTIR spectra for GF, GF-MIPs and GF-NIPs. (b) Scanning electron microscopy (SEM) images of GF, GF-MIPs and GF-NIPs.

Fig. 2a shows the FTIR spectra of the grafted fibers GF-MIPs and GF-NIPs. Compared to the spectrum of bare GF, some new bands at 2923 cm^{-1}, 2854 cm^{-1} and 1727 cm^{-1} appeared in the FTIR spectra of GF-MIPs and GF-NIPs. These bands represent the characteristics adsorption peaks of $–CH_3$, $–CH_2–$, and O=C–O, respectively, which

RSC Advances Accepted Manuscript

indicates that the polymers were successfully "grafted from" GF. Meanwhile, the morphologies of GF-MIPs and GF-NIPs were investigated by SEM. As shown in Fig. 2b, the GF substrates were coated by polymers, in contrast to the relatively smooth surface of GF. Magnified images of the GF-MIPs and GF-NIPs revealed rough surfaces that consisted of patches of polymerized protuberances. These results indicate that the polymerization process proceeded well.

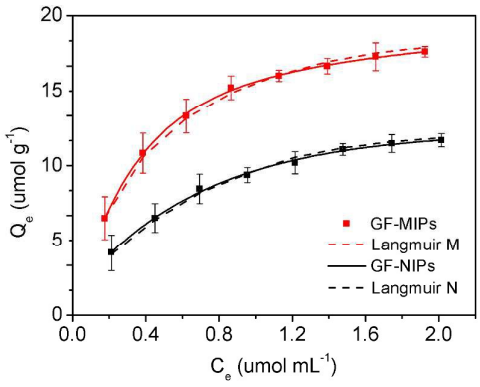

Fig. 3 Adsorption isotherms of GF-MIPs and GF-NIPs

We performed an adsorption isotherm study to evaluate the adsorption performance of the GF-MIPs and GF-NIPs. Using static binding assays, we determined that the adsorption capacities of the two samples differed substantially, as shown in Fig. 3. The nonlinear curve fitted to a one-site Langmuir binding model then yielded a perfect fit and a equilibrium constant of k = 2.38 mL·μmol^{-1} for GF-MIPs (Table 1). The GF-NIPs exhibited less affinity (k = 1.72 mL·μmol^{-1}) for the template. In addition, the Q_m for GF-MIPs (19.59 μmol·g^{-1}) was higher than that for GF-NIPs (Q_m = 12.79 μmol·g^{-1}). However, the imprinting factor of GF-MIPs was not so high (*IF* = 1.53), which indicates that many targets were adsorbed nonspecifically by the GF-NIPs, which is unfavorable for further specific adsorption.

Table 1 Langmuir isotherm constants of GF-MIPs and GF-NIPs.

	Q_m (μmol·g^{-1})	k (mL·μmol^{-1})	*IF*
GF-MIPs	19.59	2.38	1.53
GF-NIPs	12.79	1.72	

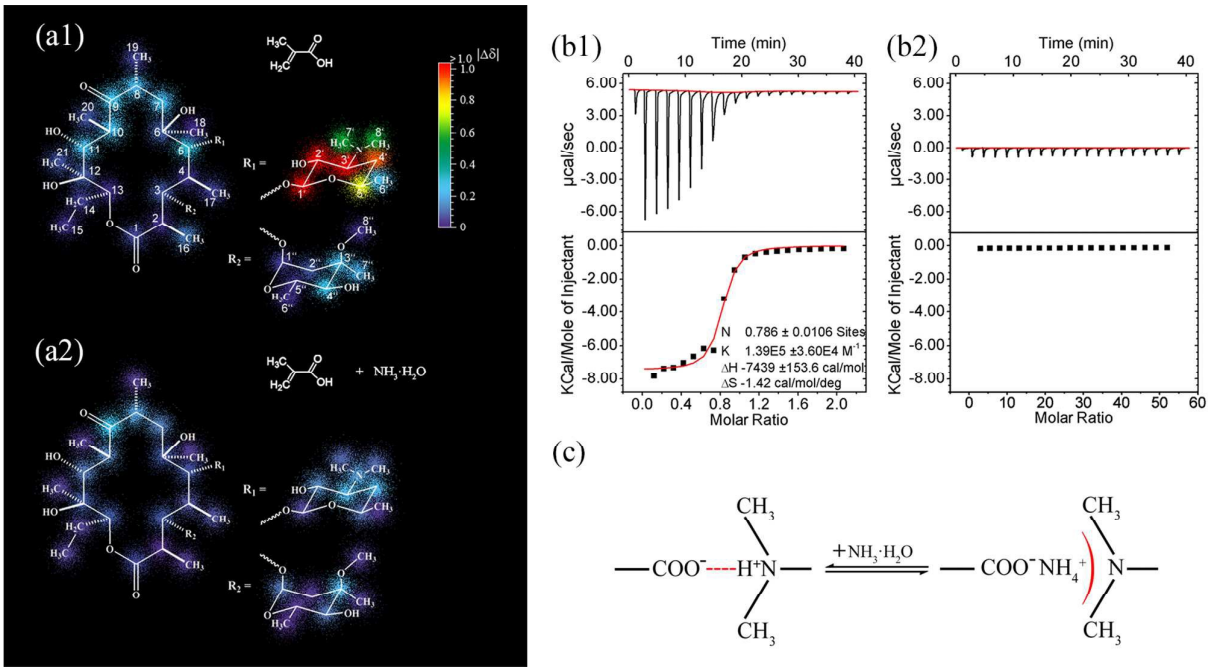

Fig. 4 (a1, a2) The absolute value of the chemical shift change (|Δδ|) of each C atom in the ERY molecular structure in the MAA binding system: (a1) $NH_3·H_2O$ free and (a2) with $NH_3·H_2O$. (b1, b2) Titration of 10 mmol·L^{-1} MAA with 1 mmol·L^{-1} ERY-A in acetonitrile/water (v/v = 6:4) at 25 °C, showing the calorimetric response as successive injections of MAA were added to the ERY-A solution: (b1) without any additional processing and (b2) with the MAA and ERY-A solution being blended with a certain amount of $NH_3·H_2O$ before titration. (c) Schematic of the variation of charged forms of the tertiary group and the –COOH group, depending on $NH_3·H_2O$.

The electrostatic interaction between the template and the fibers is likely the key point. Ionic bonds has been reported to be sufficiently strong to enable complex formation in a polar environment[14]. However, the electrostatic interaction is nondirectional[30], which would cause nonspecific binding even in MIPs with template geometry-matched cavities. ERY-A and its derivatives all contain the tertiary amine group that can accept a proton. In our previous study, we used ^{13}C-NMR measurement to demonstrate that a strong electrostatic interaction exists between the tertiary amine of ERY and the –COOH of MAA[13]. On the basis of

RSC Advances Accepted Manuscript

This journal is © The Royal Society of Chemistry 20xx

chemical shift changes of the C atoms on the ERY molecular structure when interacting with the functional monomer MAA, the strength of each binding site could be shown directly. We used the same approach to study the interaction of the two groups in a water-acetonitrile solvent. As shown in Fig. 4, $\Delta\delta$ represents the concrete values of the ^{13}C chemical shifts on ERY-A when interacting with functional monomers. Colorful spots corresponding to the absolute value of $\Delta\delta$ ($|\Delta\delta|$) on each carbon atom were pictured on the ERY-A structural formula to depict the alteration of the template magnetic environment. Fig. 4 (a1) shows that large displacements of a number of resonances arise from the C atoms (C_3', C_4', C_7', and C_8' etc.) in the vicinity of the basic tertiary amine demonstrating that the protonation of the amine group and subsequent interaction, presumably with the opposite charge corresponding to the COO^- anion, led to a substantial change in the magnetic environment of the adjacent C atoms.

Given that NH_3 can also accept a proton, we attempted to use $NH_3{\cdot}H_2O$ to block the electrostatic interaction between –COOH and the tertiary. After an appropriate amount of $NH_3{\cdot}H_2O$ was added to the solvent, the obvious chemical shifts caused by the electrostatics became extremely weak, as shown in Fig. 4(a2) suggesting that NH_4^+ interacted with $–COO^-$ and successfully prevented the interaction between the tertiary amine and the –COOH group.

Meanwhile, more direct evidence for the blocking effect of the $NH_3{\cdot}H_2O$ was provided by isothermal titration calorimetry (ITC). To investigate the contributions of electrostatic and hydrogen-bond interactions upon the formation of the MAA/ERY-A complex, the binding behavior of MAA and ERY-A were further studied by the addition of $NH_3{\cdot}H_2O$ as a blocker for the electrostatic attraction between oppositely charged MAA and ERY-A. An initial binding experiment was carried out by adding MAA to the acetonitrile/water solution of ERY-A without $NH_3{\cdot}H_2O$. Fig. 4(b1) shows the typical exothermic heat for MAA/ERY-A binding, from which the binding affinity (1.39×10^5 M^{-1}) and enthalpy (-7.4 kcal·mol^{-1}) were calculated. The molar ratio of ERY-A and MAA was just 1:1 when the exothermic heat reached equilibrium. Combining these results with the results of the ^{13}C-NMR analysis, we concluded that the tertiary amine of the ERY-A interacted with the –COOH group of MAA in a molar ratio of 1:1 and that this exothermic heating process was observable. We subsequently studied the binding behavior of MAA and ERY-A in the presence of $NH_3{\cdot}H_2O$. The $NH_3{\cdot}H_2O$ was introduced before titration, where the molar amount of NH_3 was slightly greater than the molar amount of MAA (mol:mol=1.05:1). Fig 4(b2) shows that almost no exothermic heat was observed, which clearly indicates that electrostatic interaction played a predominant role in the formation of the MAA/ERY-A complex and that the addition of $NH_3{\cdot}H_2O$ prevented the electrostatic interaction between the tertiary amine and the –COOH group. Because the useful range for an accurate binding affinity measurement by standard ITC is between 10^3 and 10^8 M^{-1}, the destabilized hydrogen bond interactions between these two small molecules in aqueous solution might be too minuscule to be detected by ITC[31].

The effect of the molar relationship between the blocker $NH_3{\cdot}H_2O$ and the –COOH incorporated into the polymers on the imprinting factor was studied. The imprinting performance of the MIPs and NIPs with various NH_3/–COOH molar ratios is presented in Fig. 5a. The binding capacity of MIPs for ERY obviously decreased with increasing NH_3/–COOH molar ratio. However, the IF increased gradually and the maximum value of more than 7 appeared at an NH_3/–COOH molar ratio of 1:1, and a slight decrease was observed when an overdosage of NH_3 was introduced. These results indicated that $NH_3{\cdot}H_2O$ prevented the electrostatic interaction between ERY and MIPs, thus inhibiting the nonspecific binding and improving the imprinting performance, also consistent with the NMR and ITC results. Then, We repeated the adsorption isotherm study in acetonitrile/water solution containing 1.05 eq. of $NH_3{\cdot}H_2O$. Similarly, the Langmuir isotherm model was also used to evaluate the adsorption behaviors of GF-MIPs and GF-NIPs. The dashed curve shown in Fig. 5 indicates that the Langmuir equation fitted well for GF-MIPs, although the maximum adsorption capacity (Q_m) was significantly decreased (Table 2). For non-imprinting fibers, the adsorption capacity over the entire range of concentrations was close to zero, and the binding isotherm could not be adequately fit using the Langmuir model because of the large margin of error. Thus, we regarded the Q_e of GF-MIPs at a concentration of 2.18 μmol·mL^{-1} as an approximate Q_m value. Although the Q_m values of both of the two fibers decreased, their *IF* values increased significantly by a factor of approximately 7.58. The GF-MIPs exhibited a remarkably good imprinting effect.

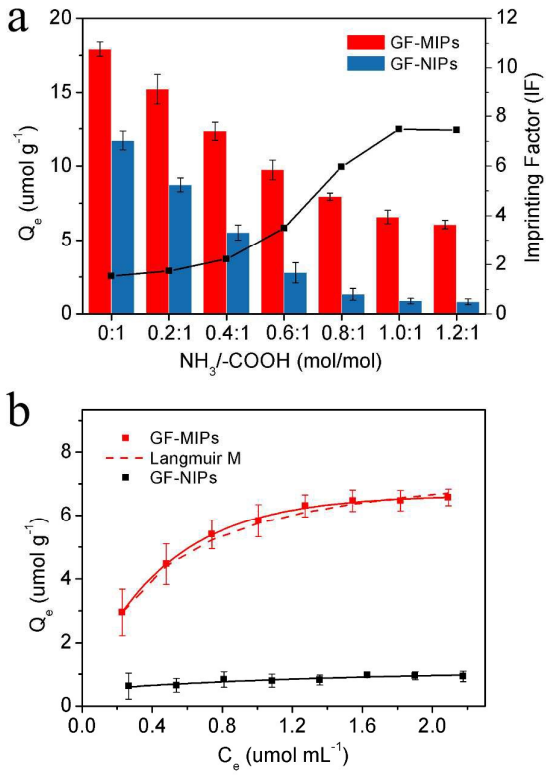

Fig. 5 (a) The effect of the molar relationship between the $NH_3{\cdot}H_2O$ blocker and –COOH on the imprinting factor; initial concentration: 2.37

RSC Advances Accepted Manuscript

μmol·mL^{-1}. (b) Adsorption isotherms of GF-MIPs and GF-NIPs with additional $NH_3 \cdot H_2O$.

Table 2 Langmuir isotherm constants of GF-MIPs and GF-NIPs with additional $NH_3 \cdot H_2O$.

	Q_m (μmol·g^{-1})	k (mL·μmol^{-1})	*IF*
GF-MIPs	7.35	2.56	7.58
GF-NIPs	≈0.97	~	

The selectivity tests of GF-MIPs were carried out under equilibrium binding conditions by using KANA and DEX as contrasting adsorbates. Their chemical structures are shown in Fig. 1. The equilibrium adsorption capacity (Q_e) and the distribution coefficient (K_D) of the selected adsorbates between the solution and the fibers are shown in Fig. 6. K_D is defined as

$$K_D = \frac{Q_e}{C_e} \quad (3)$$

where Q_e (μmol·g^{-1}) and C_e (μmol·mL^{-1}) are the equilibrium concentration of ERY-A on the adsorbent and in solution, respectively.

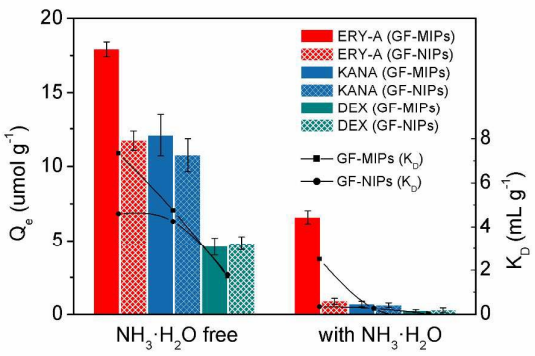

Fig. 6 Q_e and K_D of adsorbates on GF-MIPs and GF-NIPs under equilibrium binding conditions. Concentrations of the starting solution are all 2.73 μmol·mL^{-1}.

As shown in Fig. 6, the amount of ERY-A adsorbed onto GF-MIPs with a value of 17.99 μmol·g^{-1}, was much higher than the amounts of other adsorbates. After a balanced amount of $NH_3 \cdot H_2O$ was added, the adsorbed amount of ERY-A, 6.58 μmol·g^{-1}, was still the highest among all adsorbates (even though its adsorption capacity decreased). The calculated values of the distribution coefficients K_D exhibited the same trend. The K_D values of GF-MIPs for ERY-A were observed to be the highest for both "$NH_3 \cdot H_2O$ free" and "$NH_3 \cdot H_2O$ containing" groups: 7.33 mL·g^{-1} and 2.51 mL·g^{-1}, respectively. GF-MIPs exhibited better adsorption capacity for the template than all of the other adsorbates. GF-MIPs still adsorbed large amounts of of KANA in the test group without $NH_3 \cdot H_2O$, even though the amounts of KANA adsorbed onto GF-MIPs and GF-NIPs were not drastically different. However, in the group with additional $NH_3 \cdot H_2O$, there was little KANA adsorbed by GF-MIPs and GF-NIPs. Because KANA contains four amino groups, we speculated that the electrostatic interactions between these amino and –COOH groups on the fibers led to nonspecific adsorption. After sufficient $NH_3 \cdot H_2O$ was added to form a barrier to the electrostatic interaction, the amount of KANA adsorbed plunged because of the lack of corresponding imprinting cavities as well as the lack of electrostatic interaction. Understandably, very little DEX, which does not contain any nitrogen-containing radicals, was adsorbed onto the two fibers in both the $NH_3 \cdot H_2O$-containing solution and the $NH_3 \cdot H_2O$-free solution. These results indicate that the imprinting fibers possessing microcavities with a good memory for the template work well in our acetonitrile/H_2O system, where $NH_3 \cdot H_2O$ can deactivate the –COOH and thus result in excellent specific adsorption performance. After $NH_3 \cdot H_2O$ was added, even in the presence of hydrophobic interaction, these contradistinctive adsorbates had no complementary shapes with the imprinting cavities of GF-MIPs, thus resulting in little adsorption.

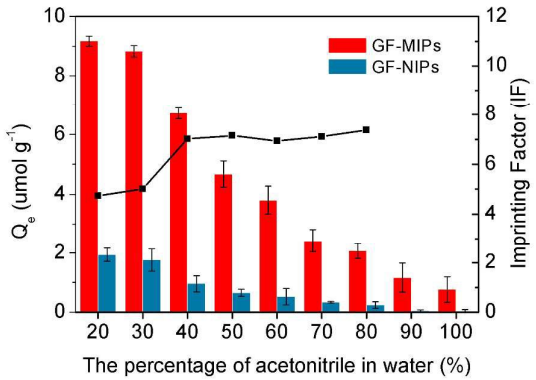

Fig. 7 Adsorption capacity and imprinting factors of GF-MIPs and GF-NIPs in acetonitrile/water solutions with percentage compositions of acetonitrile ranging from 20% to 100% and containing 0.1% $NH_3 \cdot H_2O$; initial concentration: 2.73 μmol·mL^{-1}.

The nature of the solvent used for the adsorption experiment is also known to influence the imprinting effect of the MIPs. This effect is quite complicated for aqueous solutions[32,33]. In general, a higher percentage of water can provide more hydrophobic solvent conditions for interaction. Because, hydrophobic interactions are nondirectional, they are detrimental to the specificity but can provide the power of adsorption[34]. Discerning whether the hydrophobic interaction is benefit is difficult. Moreover, in the presence of polar solvents, particularly water, the theoretical H-bond interactions between solutes and adsorbents are destabilized[35,36]. Therefore, we performed static adsorption experiments with $NH_3 \cdot H_2O$ in acetonitrile-water solvents with percentage compositions of acetonitrile ranging from 20% to 100% (given the solubility of ERY). We then calculated the adsorption capacities of GF-MIPs and GF-NIPs for ERY-A using HPLC detection. Recent studies have shown that noncovalent imprinted polymers has been used mostly in the presence of polar solvents, especially water, to satisfy the requirements of applications; these solvents severely disturb the interactions based on hydrogen bonding among the molecules. Interactions such as ionic bonds and hydrophobic interactions, the predominant interactions in aqueous solution, have been suggested to be sufficiently strong to allow for specific

RSC Advances Accepted Manuscript

This journal is © The Royal Society of Chemistry 20xx

adsorption in a polar solution[37,38]. For our system, hydrogen bonds were also destabilized in acetonitrile/water solution and ionic bonds were hardly existent because of the blocking effect. Therefore, the imprinting mechanism here might be more complicated. Though simple hydrophobic interactions are generally nonspecific, these interactions are strong in aqueous solution and should thus make a critical contribution to adsorption. The complementary imprinting voids that match the steric structure of the template are presumed to provide the specificity of adsorption. The mechanism of this specific adsorption based on the combination of hydrophobic and other non-electrostatic interactions is not entirely clear; however, the literature contains numerous studies that demonstrate that noncovalent imprinted polymers exhibit good imprinting efficiency in aqueous solutions, without the benefit of electrostatic interactions[39,40].

All results are shown in Fig 7. Overall, the results indicated that the adsorbed amount of ERY-A tends to decrease with increasing percentage of acetonitrile in solutions because of the weakening of the hydrophobic interaction between GF-MIPs and ERY-A caused by the increasing proportion of the organic solvent. With low percentages of acetonitrile—20% and 30%—GF-MIPs exhibit a high binding capacity for ERY-A; however, the IF values were relatively low, because strong hydrophobic interactions under these conditions caused undesired nonspecific adsorption. When the percentage of acetonitrile was increased to 40%, the specificity of GF-MIPs for ERY-A had begun to manifest. In this case, the *IF* value increased to 7.14. We also observed that the IF values remained approximately the same as those of the solutions that contained more than 40% of acetonitrile (the *IF* values in 90% and 100% acetonitrile solutions could not be calculated because the Q_e values of the GF-NIPs in these solutions were close to zero). Under these conditions, the specificity of the GF-MIPs for ERY-A did not change significantly with increasing acetonitrile percentage. These hydrophobic interactions and steric shape might explain why the specificity of GF-MIPs for the template did not significantly change as the percentages of acetonitrile was varied from 40% to 80%. On the whole, we chose the 40% acetonitrile-water solution as the mobile phase for further dynamic adsorption experiments considering both specificity and adsorption capacity of GF-MIPs.

To investigate the selectivity of GF-MIPs, competitive adsorption experiments were performed in a solution of ERY-A, ERY-E and ERYee standards (molar ratio = 5:3:2, which is similar to the molar ratio of the crystal mother liquid). Fig. 8 shows the binding quantity of the three ERY imprints and those for their corresponding non-imprinted control samples. In the absence of $NH_3{\cdot}H_2O$, the GF-MIPs adsorbed much more ERY-A and other ERY-derivatives than GF-NIPs at each concentration. However, no differences were observed in the adsorption of GF-MIPs for these three ERY samples. GF-MIPs showed little specificity toward ERY-A while using structurally similar substances as competitive adsorbates. After the blocker was added, a comparison of the binding capacity of GF-MIP for different ERY samples revealed that $NH_3{\cdot}H_2O$ substantially influenced the selectivity. The binding of a relatively large quantity of ERY-A was achieved, and the binding performances of NIPs for various ERY were all poor, showing no difference. These results suggest that $NH_3{\cdot}H_2O$ as a blocker can effectively block nonspecific adsorption and improve the selectivity of the GF-MIPs.

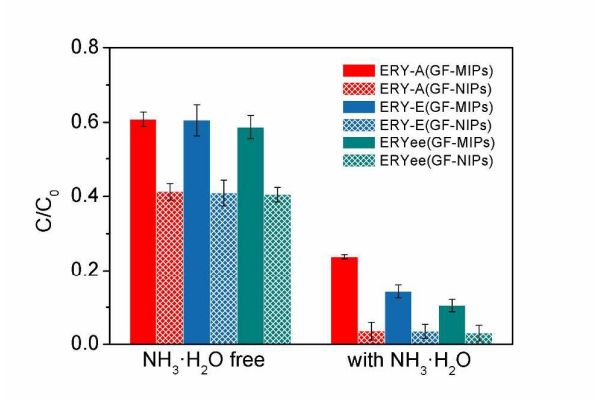

Fig. 8. Adsorption capacity of GF-MIPs and GF-NIPs for ERY-A, ERY-E and ERYee. Total concentration of all three ERY: 2.73 μmol·mL^{-1}.

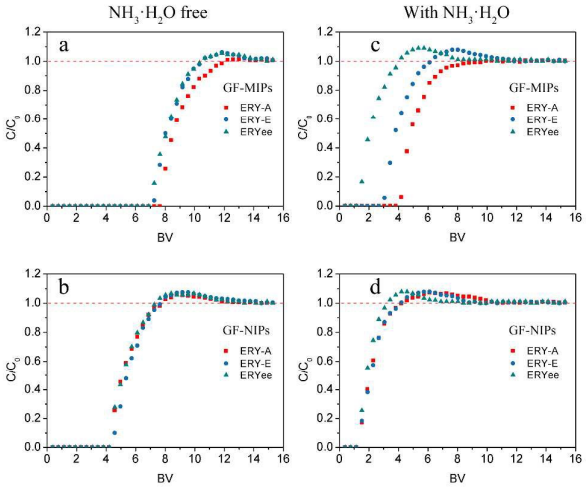

Fig.9 Breakthrough curves of a GF-MIPs bed column and a GF-NIPs bed column; flow rate: 0.31 BV·h^{-1}; solution: 40% acetonitrile in water; (a) and (b) $NH_3{\cdot}H_2O$ free; (c) and (d) with 0.1% $NH_3{\cdot}H_2O$.

A competitive adsorption study in a dynamic experiment model was performed to provide more robust evidence for template selective binding and to demonstrate the potential application in the ERY recovery from the ERY crystal mother liquid. In this study, we dissolved (in acetonitrile/water) the powder that we obtained by drying the "ERY crystal mother solution". Then, these solutions (with or without $NH_3{\cdot}H_2O$) continued to flow through the chromatographic columns that composed with the GF-MIPs or GF-NIPs bed. Meanwhile, the effluents were collected at regular intervals and the concentrations of the three analytes (ERY-A, ERY-E, ERYee) at each point were detected by HPLC. Fig. 8 shows that, as the solution passed through the column, ERY-A, ERY-E and ERYee all clearly flowed from the GF-MIPs column later than they flowed from the GF-MIPs column, both in the case of the "with $NH_3{\cdot}H_2O$" group and in the case of the "$NH_3{\cdot}H_2O$ free" group. Obviously, the GF-MIPs exhibited better adsorption properties

RSC Advances Accepted Manuscript

for ERY-A and its derivatives in the dynamic adsorption process. However, even the GF-MIP column could hardly separate the three very similar compounds (Fig. 9a). As we previously discussed, the adverse effects of the electrostatic interactions severely hindered the molecular recognition. A strong electrostatic interaction masked other interactions, and this electrostatic interaction existed between MAA and both ERY derivatives. Thus, fine separation for ERY-A from its derivatives using GF-MIPs directly is difficult, even when employing a dynamic model. Therefore, the "blocker", $NH_3 \cdot H_2O$, was also added during the dynamic adsorption process. Fig. 9c shows the breakthrough curve of ERY-A, ERY-E and ERYee in the GF-MIPs column after $NH_3 \cdot H_2O$ was added to the solutions. The breakthrough times of all three samples clearly differed. The leaking volume of ERY-A was estimated to be 4.2 BV, whereas those for ERY-E and ERYee were estimated to be 2.5 BV and 1.4 BV, respectively. During this process, ERY-A and other derivatives maintained a dynamic process of adsorption and desorption. Because the GF-MIPs bed had specificity for ERY-A, the intensities of interactions between the column and various ERY differed. Thus, these results show that the GF-MIPs bed column has good selectivity and specificity for ERY and tends to adsorb ERY-A preferentially over other derivatives under a dynamic condition. The dynamic binding test again demonstrated the effectiveness of employing $NH_3 \cdot H_2O$ as a blocker to block the electrostatic interaction and improve the imprinting efficiency, which exhibits attractive application prospects for the precise separation of ERY-A from its recrystallization wastewater.

Conclusion

The facile preparation of surface molecular imprinted polymers on glass fibers is presented in this work. The major problem with selective recognition lies in the nonspecific interaction between adsorbents and adsorbates. To optimize the selectivity of MIPs, ^{13}C-NMR and ITC were employed to confirm that the strong electrostatic interaction between tertiary amine groups and –COOH groups led to the undesired nonspecific adsorption, which can be effectively suppressed by the addition of $NH_3 \cdot H_2O$. The as-prepared GF-MIPs provided resistance to nonspecific structural analogs' adsorption and specificity toward ERY-A in the presence of $NH_3 \cdot H_2O$. Successful application to the selective enrichment of ERY-A from a ERY crystal mother solution suggested that the GF-MIPs could be an alternative solution for precise ERY separation. Moreover, our work demonstrated the feasibility and significance of mediating the solvent environment to increase recognition capability and achieve accurate separation.

Acknowledgements

We acknowledge the financial support from Shanghai Natural Science Foundation (11ZR1409100), the National Natural Science Foundation of China (5110304, U1024209), the National Basic Research Program of China (973 Program, 2012CB933600), Innovation Program of Shanghai Municipal Education Commission (14ZZ060), the Fundamental Research Funds for the Central Universities (WD1214056) and Outstanding Youth Fund of East China University of Science and Technology (YD0157109).

Notes and references

1 W. H. Pirkle and T. C. Pochapsky, Chem. Rev., 1989, 89, 347–362.
2 N. M. Maier, P. Franco and W. Lindner, J. Chromatogr. A, 2001, 906, 3–33.
3 M. Yoshikawa, A. Shimada and J. Izumi, Analyst, 2001, 126, 775–780.
4 X. Dong, H. Sun, X. Lu, H. Wang, S. Liu and N. Wang, Analyst, 2002, 127, 1427–1432.
5 N. Cabaleiro, I. de la Calle, C. Bendicho and I. Lavilla, Anal. Methods, 2013, 5, 323–340.
6 C. D. Bevan and P. S. Marshall, Nat. Prod. Rep., 1994, 11, 451–466.
7 Y. Li, N. Wang, M. Zhang, Y. Ito, H. Zhang, Y. Wang, X. Guo and P. Hu, Anal. Chem., 2014, 86, 3373–3379.
8 R. Olmedo, V. Nepote and N. R. Grosso, Food Chem., 2014, 156, 212–219.
9 L. Chen, S. Xu and J. Li, Chem. Soc. Rev., 2011, 40, 2922–2942.
10 S. Xu, H. Lu, X. Zheng and L. Chen, J. Mater. Chem. C, 2013, 1, 4406–4422.
11 A. Derazshamshir, F. Yilmaz and A. Denizli, Anal. Methods, 2015, 7, 2659–2669.
12 A. Hassanzadeh, P. a Gorry, G. a Morris and J. Barber, J. Med. Chem., 2006, 49, 6334–42.
13 Y. Zhang, X. Qu, J. Yu, L. Xu, Z. Zhang, H. Hong and C. Liu, J. Mater. Chem. B, 2014, 2, 1390–1399.
14 K. Haupt, A. Dzgoev and K. Mosbach, Anal. Chem., 1998, 70, 628–631.
15 Y. Zhang, D. Song, L. M. Lanni and K. D. Shimizu, Macromolecules, 2010, 43, 6284–6294.
16 R. D. Rasberry and K. D. Shimizu, Org. Biomol. Chem., 2009, 7, 3899–3905.
17 Y. Zhang, D. Song, J. C. Brown and K. D. Shimizu, Org. Biomol. Chem., 2011, 9, 120–126.
18 A. B. Pun, K. J. Gagnon, L. M. Klivansky, S. J. Teat, Z.-T. Li and Y. Liu, Org. Chem. Front., 2014, 1, 167–175.
19 R.-T. Ma and Y.-P. Shi, Talanta, 2015, 134, 650–656.
20 L. A. de Barros, L. A. Pereira, R. Custódio and S. Rath, J. Braz. Chem. Soc., 2014, 25, 619–628.
21 B. Iacob, E. Bodoki and R. Oprean, Electrophoresis, 2014, 35, 2722–2732.
22 T. Pap, V. Horváth, A. Tolokán, G. Horvai and B. Sellergren, J. Chromatogr. A, 2002, 973, 1–12.
23 Y. Kondo and M. Yoshikawa, Analyst, 2001, 126, 781–783.
24 N. W. Turner, E. V Piletska, K. Karim, M. Whitcombe, M. Malecha, N. Magan, C. Baggiani and S. A. Piletsky, Biosens. Bioelectron., 2004, 20, 1060–1067.
25 A. Matsumoto, K. Tsutsumi, K. Schumacher and K. K. Unger, Langmuir, 2002, 18, 4014–4019.
26 B. Song, Y. Zhou, H. Jin, T. Jing, T. Zhou, Q. Hao, Y. Zhou, S. Mei and Y.-I. Lee, Microchem. J., 2014, 116, 183–190.
27 S. Song, A. Wu, X. Shi, R. Li, Z. Lin and D. Zhang, Anal. Bioanal. Chem., 2008, 390, 2141–2150.
28 B. B. Prasad, A. Srivastava and M. P. Tiwari, J. Colloid Interface Sci., 2013, 396, 234–41.
29 S. Lépinay, A. Ianoul and J. Albert, Talanta, 2014, 128, 401–7.
30 P. Anzenbacher, K. Jursikova, D. Aldakov, M. Marquez and R. Pohl, Tetrahedron, 2004, 60, 11163–11168.

RSC Advances Accepted Manuscript

This journal is © The Royal Society of Chemistry 20xx

31 B. W. Sigurskjold, Anal. Biochem., 2000, 277, 260–266.
32 V. Pakade, S. Lindahl, L. Chimuka and C. Turner, J. Chromatogr. A, 2012, 1230, 15–23.
33 H. Zhang, Polymer., 2014, 55, 699–714.
34 A. Ustinov, H. Weissman, E. Shirman, I. Pinkas, X. Zuo and B. Rybtchinski, J. Am. Chem. Soc., 2011, 133, 16201–16211.
35 H. Yan, M. Wang, Y. Han, F. Qiao and K. H. Row, J. Chromatogr. A, 2014, 1346, 16–24.
36 S. Xu, H. Lu and L. Chen, J. Chromatogr. A, 2014, 1350, 23–29.
37 L. I. Andersson, Anal. Chem., 1996, 68, 111–117.
38 J. O'Mahony, A. Molinelli, K. Nolan, M. R. Smyth and B. Mizaikoff, Biosens. Bioelectron., 2005, 20, 1884–1893.
39 W. Wei, R. Liang, Z. Wang and W. Qin, RSC Adv., 2015, 5, 2659–2662.
40 H. Shaikh, M. Andaç, N. Memon, M. I. Bhanger, S. M. Nizamani and A. Denizli, RSC Adv., 2015, 5, 26604–26615.

RSC Advances Accepted Manuscript

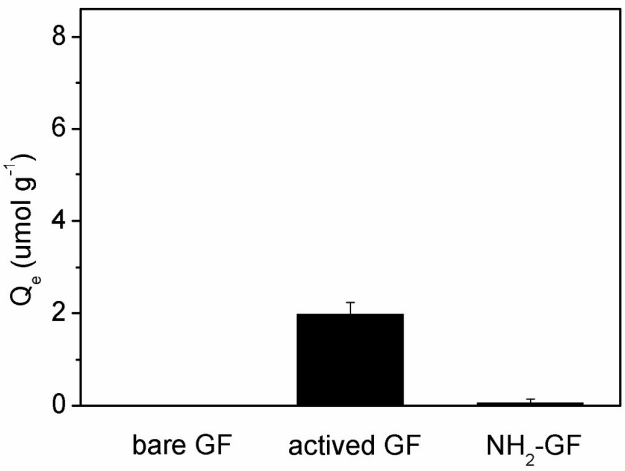

Fig. S1 Adsorption capacities of different GF for ERY. Bare GF: glass fibers without any preprocessing; active GF: glass fibers activated by a hot alkali solution; NH_2-GF: amino-modified GF using a silane coupling agent.

RSC Advances Accepted Manuscript